Hemoglobin adsorption isotherm at the silica-water interface with evanescent wave cavity ring-down spectroscopy

W. Blake Martin
University of Alabama at Birmingham
Department of Biomedical Engineering
1075 13th Street South, Suite 370
Birmingham, Alabama 35294-4440
E-mail: bmeblake@uab.edu

Sergey Mirov
Dmitri Martyshkin
University of Alabama at Birmingham
Department of Physics
1300 University Boulevard
Room 310, Campbell Hall
Birmingham, Alabama 35294-4440

Ramakrishna Venugopalan
A J&J Company
Neuro Modulation Research and Development
Codman and Shurtleff
325 Paramount Drive
Raynham, Massachusetts 02767-0350

Andrew M. Shaw
University of Exeter
School of Biological and Chemical Sciences
Stocker Road
Devon, United Kingdom EX4 4QD

Abstract. Evanescent wave cavity ring-down spectroscopy (EW-CRDS) is used to observe the adsorption isotherm for hemoglobin (Hb) from controlled urine samples to assess the potential for rapid diagnosis in hemoglobinuria. The absorbance of Hb at 425 nm is monitored using an alexandrite laser-pumped, room temperature, LiF:F_2^{+**} color-center pulsed laser. A minimum absorbance detection level of 2.57×10^{-4} is achieved, corresponding to a minimum detectable concentration of Hb in urea of 5.8 nM. A multilayered Hb biofilm is formed, and a minimum of eight layers are required to model the adsorption isotherm, allowing for cooperative binding within the layers and extending 56 nm into the interface. A binding constant for Hb to silica $18.23\pm7.58\times10^{6}$ M is derived, and a binding constant for Hb to Hb in subsequent layers is determined to be $5.631\pm0.432\times10^{5}$ M. Stoichiometric binding coefficients of 1.530 ± 0.981 for layer one and 1.792 ± 0.162 for subsequent layers suggest that cooperative binding both to the silica surface and between the layers of the biofilm is important. [DOI: 10.1117/1.1891368]

Keywords: evanescent wave cavity ring-down spectroscopy; hemoglobin; adsorption; isotherm; spectroscopy; modeling.

Paper 04066 received May 4, 2004; revised manuscript received Aug. 19, 2004; accepted for publication Oct. 26, 2004; published online; published online Apr. 29, 2005.

1 Introduction

Direct optical absorption methods are commonly used to monitor molecules in biological solutions[1] based on the accurate monitoring of the change in transmitted light intensity. Evanescent wave cavity ring-down spectroscopy (EW-CRDS) is an ultrasensitive absorption spectroscopy with an internal calibration that provides absolute measures of absorbance with sensitivities typically of order 10^{-4}. This work explores the application of EW-CRDS to the detection of Hb in urea by direct optical absorption to investigate the potential for early diagnosis of the medical condition hemglobinurea. The strong absorption of Hb at 425 nm is used to measure the spectrum of Hb during the formation of a biofilm at the silica-water interface. Absorbance measurements are also used to monitor the Hb biofilm formation, and the resulting adsorption isotherm is modeled using a cooperative binding analysis of the data.

Optical techniques in general suffer from nonspecific absorbance specificity, which is overcome conventionally by tagging a fluorophore to the analyte and interrogating the solution with fluorescence spectroscopy. With this method, a fluorophore of known and specific affinity for the target analyte is added to the sample, and the fluorescence is monitored as a function of analyte concentration. Recent studies by Tolosa et al. have demonstrated the use of the fluorophore RuCon A as a selective binding agent for glucose to determine the sugar level for diabetics.[2] The assay contained a fluorophore that binds to the maltose and malachite green insulin compound (MIMG). The glucose molecules competitively bind in the place of maltose. The glucose binding disrupted the MIMG and RuCon A binding, liberating RuCon A into solution. Excitation at 460-nm light showed fluorescence with a decay lifetime sensitive to the competitive binding of glucose to the fluorophore complex. All fluorescence techniques are, however, vulnerable to the presence of species in a complex biofluid, which may inhibit or quench fluorescence from the fluorophore and lead to a false concentration determination, yielding particular problems from any fluorophore-based assay for implantable devices.[2]

Many biological analytes have been explored over recent years with the use of optical absorption methodologies. Glucose is a frequently researched molecule because of the need to monitor and control its levels for diabetics. Optical detection of analytes has used many techniques, including infrared absorption for glucose in serum,[3] Raman spectroscopy, polarimetry, and fluorescence.[4] A new ultrasensitive absorption technique offers increased sensitivity to target species and immunity from fluorescence quenching.

Address all correspondence to William Blake Martin, Medtronic Sofamor Danek Distributor, Medicraft, Inc., 3290 Northside Parkway - Suite 330, Atlanta, GA 30327. Tel: 800-767-6401; Fax: 205-975-4919; E-mail:bmartin@medicraft.com

1083-3668/2005/$22.00 © 2005 SPIE

Cavity ring-down spectroscopy (CRDS) is the study of analytes in an optical cavity resonator. The use of an optical cavity and the resultant photon decay time of the radiation intensity within the cavity have been explored previously.[5] In the late 1980's, O'Keefe and Deacon were the first to use optical cavities to determine the absorption spectra of gaseous samples,[6] and this has since been extended to many regions of the electromagnetic spectrum.[7–9] The most sensitive direct absorbance measurements have been made using continuous laser (cw) sources[10,11] with absorbance sensitivities of order $5 \times 10^{-8}\,\mathrm{cm}^{-1}$ achieved that approach the shot-noise limited sensitivity of order 10^8 molecules/cm^3. Many reviews of the technique and its developments have been published elsewhere.[7,12–14]

Simply put, an optical cavity is created between two highly reflective mirrors that trap a pulse of laser radiation within the cavity. A small amount of radiation leaks out from the cavity on reflection from each mirror, and as a result a light pulse is reflected back and forth through the cavity many thousands of times. The decay rate of the light intensity in the cavity depends on the Q of the cavity, and for high-reflectivity mirrors the decay rate is exponential with a decay constant τ of several tens of microseconds. When a gaseous sample, which absorbs at the wavelength of the laser radiation, is introduced into the cavity, the quality of the cavity drops, and the ring-down time decreases. The change in ring-down time is related to the wavelength-dependent extinction coefficient of the molecule, and if this is known, an absolute concentration determination is possible. The potential benefits of this system are quickly seen when compared to simple optical transmission systems. For the single-pass transmission system, light interacts with the sample for a defined length, one-pass, whereas in the optical cavity, the effective path of the light can often be 10,000 times the cavity length, a path length of 10 km.

Introduction of a gas phase species into the cavity results in additional losses within the cavity dominated by molecular absorption. However, the radiation scatter from a droplet or liquid sample significantly reduces the number of passes through the sample and hence the sensitivity. CRDS has been applied successfully to condensed phase samples and hence has the potential for biomedical analyte analysis, although direct path propagation in water is problematic. Several techniques have begun to explore the usefulness of CRDS to condensed materials.[15–18] Direct incorporation of the liquid into the cavity can result in useful measurements within the liquid, but care has to be taken to choose the liquid carefully to minimize absorption and physical disturbances, such as turbulence and thermal lensing.[19,20] In the case of very short ring-down times, each pulse of the laser radiation can be detected by visualizing the pulse train bounce by bounce, and this has been applied to ultrafast dynamics within liquids.[21]

Recent condensed phase absorption studies have implemented the simple use of a total internal reflection method by introducing a Dove prism into the cavity.[22] The Dove prism configuration allows the region within 200 nm of the silica prism surface to be investigated but preserves the optical quality of the cavity. The configuration allows some 500 passes through the sample and has demonstrated absorbance sensitivity of order 10^{-5}. The EW-CRDS technique has potential application to biological questions of biofilm formation[23] either naturally or in the propagation of disease, in particular understanding the biofilm formation as a function of the surface properties. The strong visible absorption spectrum of Hb makes this molecule an ideal prototype for monitoring biofilm formation and is chosen for this study.

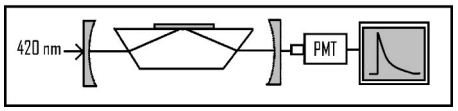

Fig. 1 The schematic diagram of the experimental apparatus is displayed.

Hemoglobinuria is a clinical condition in which abnormally high levels of Hb are present in the urine. Early diagnosis of hemoglobinuria requires low concentrations of the Hb to be detected, as healthy individuals should have no detectable trace of blood in the urine. Current dipstick methods have limited sensitivity and give only false/positive tests. EW-CRDS-based techniques offer the potential to reduce the detection limits and diagnose the onset of the condition more rapidly, providing real-time quantitative information on the hemoglobin concentration.

This work reports EW-CRDS studies of Hb adsorption to the silica surface from solutions of known concentrations of Hb in controlled urine samples. The study establishes a detection sensitivity limit and determines the adsorption isotherm of the Hb protein to the silica surface. A competitive binding model of the isotherm will be fitted to the experimental data to understand the interaction between Hb and the silica surface and subsequent Hb-Hb layers. Estimated binding constants and stoichiometric binding coefficients are also determined.

2 Experimental

The measurements of the Hb adsorption isotherm were made with a similar EW-CRDS configuration described in detail elsewhere[15–18,22] and shown schematically in Fig. 1. It is described only briefly here. Two high reflectivity mirrors (99.995%, radius of curvature 6 m, Los Gatos Research, Mountain View, California) are aligned optically opposite one another to form a stable optical resonator of length 1.1 m. An alexandrite laser-pumped, room temperature, LiF:F_2^{+**} color-center pulsed laser was used to generate radiation tunable from 410 to 605 nm after frequency doubling, with a 50-ns pulse duration, a 10-Hz repetition rate, and an average energy output per pulse of 0.5 mJ.[24] The pulsed laser is introduced into the cavity through the front mirror and makes many roundtrips through the cavity. At each bounce with the mirror, some radiation is lost to the cavity and the radiation intensity decays with time. The intensity decay is detected behind the second mirror with a high-speed, gated visible-ultraviolet photomultiplier detector (H7680-01, Hamamatsu Photonics, Hamamatsu, Japan) and digitized on a Tektronix TDS5104 oscilloscope (1-GHz sampling rate, Tektronix, Beaverton, Oregon).

The exponential decay of the radiation is formally the decay from several cavity modes that are excited within the bandwidth of the pulsed radiation. The ring-down τ is hence an estimate of all mode ring-down times, but the differences are assumed to be small and the representation of the radiation

decay as a single exponential is a good practical approximation. The trace is averaged over 64 laser shots and fitted to a single exponential using a nonlinear Levenberg-Marquart fitting routine. The resulting exponential decay is characterized by a ring-down time τ, which for an empty cavity at 420 nm was found to be 3.5 μs with a variation $\sigma\tau/\tau$ of order 1%.

A dove prism (Lambda Research Optics, Costa Mesa, California) was introduced into the cavity equidistant from the mirrors with a transmittance for *p*-polarized light at 420 nm of 99.371%, as reported by Lambda Research Optics, determined by the quality of the antireflection coatings on the prism. The Q of the dove cavity was reduced and the ring-down time decreased to typically 200 ns with an uncertainty $\sigma\tau/\tau$ of order 2%. The dove prism configuration preserves the path of the radiation within the cavity and introduces a total internal reflection (TIR) event at the back surface of the prism. TIR results in the generation of an evanescent wave at the surface with an electric field that decays exponentially into the medium above the prism with a penetration depth d_p, determined by:

$$d_p = \frac{\lambda}{2\pi n_1 \{[\sin(\vartheta)]^2 - n_{21}^2\}^{1/2}}, \tag{1}$$

where λ is the wavelength of the radiation propagating in the prism, θ is the angle of incidence at the interface with respect to the normal, n_1 is the refractive index of the prism, and n_{21} is the ratio of the refractive index of the sample and the refractive index of the prism (1.4677 at 425 nm, Lambda Research Optics). For the configuration shown in Fig. 1, the penetration depth is $\sim$163 nm.

The radiation explores an elliptical area on the back surface of the prism, which at the center of the cavity is a measure of the area of the beam waist for the cavity modes W_0. For symmetric resonators, the beam waist is given by:

$$W_0^2 = \left(\frac{L\lambda}{\pi}\right)\left[\frac{(1+g)}{4(1-g)}\right]^{1/2}, \tag{2}$$

where L is the length between the two mirrors, λ is the wavelength of the radiation, and $g = 1 - L/R$, with R being the radius of curvature of the mirrors. The laser beam profile for the incoming radiation was measured using a laser beam analyzer (Model LBA-100, Spiricon, Logan, Utah) and found to be 0.407 mm, which is smaller than the calculated beam waist for a 1.1-m cavity, or 0.484 mm. The errors in determining the ring-down time are reduced when the measured beam waist outside the cavity is matched to the optical cavity mode beam waist W_0, and this is achieved by external, precavity optics. Stability improvements in τ, $\sigma\tau/\tau$, were also obtained when the excitation beam waist matched the cavity mode.

Molecules present within the beam-waist footprint and evanescent field on the back of the prism can absorb at the wavelength of the laser radiation and thus remove energy from the evanescent field. Absorption from the evanescent field constitutes an additional loss in the cavity and reduces the ring-down time τ. The change in τ can be used to calculate the absorbance due to the molecules and is given by:

$$\text{abs} = \frac{\Delta\tau}{\tau_0 \tau}\left(\frac{t_r}{2}\right), \tag{3}$$

where τ_0 is the ring-down time for the empty cavity, $\Delta\tau$ is the change in τ due to the molecular absorbance, and t_r is the roundtrip time of the cavity, including the propagation of the radiation through the prism material. The absorbance is converted to base 10 logarithms by multiplying by 2.303, to be consistent with the definition of the extinction coefficient ϵ. Typically, variation in recorded τ values produced a percentage error of order $\sim$1% in a ring-down time of 200 ns, producing a minimum absorbance detection limit of 2.57×10^{-4}.

It can be seen from Eq. (3) that the absorbance measurement depends on the change in the ring-down time τ, and is independent of the intensity of the radiation in the cavity. Hence, CRDS is intrinsically immune to the fluctuations in the laser source intensity. Further, the careful calibration of the time scale in the experiment by the digital oscilloscope enables an absolute measure of the absorbance to be determined without the need for absorption calibration standards.

The liquid sample was introduced to the surface of the dove prism with a custom-made sample holder allowing a clear optical path through the prism. Plastic barriers were mounted to the top surface to contain the sample and ensure complete coverage of the evanescent field. An exit channel was made to send the rinsed fluids away from the setup to a glass beaker. The rinsed fluids traveled perpendicular with respect to the laser beam propagation. The surface was cleaned and dried with compressed air before the sample was placed on the surface of the dove prism.

The background ring-down time τ_0 was recorded with a deionized, distilled water blank sample and further washed with the blank urine control sample; neither had a significant change in τ. The urine sample was a MAS® urinalysis liquid assayed normal control (Fisher Scientific, Pittsburgh, PA) and was used as the solvent for all solutions. The composition of the MAS® was: bilirubin (0 mg/dl), no blood, creatinine (10 to 50 mg/dl), glucose (120 to 100 mg/dl), no hCG, no ketones, no leukocytes esterase, microalbumin (10 mg/L), nitrite (400 to 600 mOsm), potassium (20.9 to 21.9 mEq/L), no protein, no red blood cells, sodium (295 to 315 mEq/L), urobilinogen ($<$1 mg/dl), and white blood cells (1 to 10 per μL). Dried hemoglobin (Fisher Scientific, Pittsburgh, PA) was added in known quantities to the urine sample and stirred until completely dissolved. After τ_0 was recorded for the deionized, distilled water, the surface was cleaned and dried with compressed air. A 200-μL sample was added to the surface, ensuring complete coverage of the beam-waist footprint. The change in τ was observed over time intervals from 0.5 to 30 min, during which time the sample did not dry out. The prism was cleaned between experiments with alternate washes of distilled water, 0.1-M NaOH and 0.1-M HCl, until the background ring-down time τ_0 recovered to its initial value. Hemoglobin was added to the control urine sample over a concentration range of 0 to 12 μM (0 to 75 mg/dl) and the equilibrium adsorption isotherm recorded at each concentration.

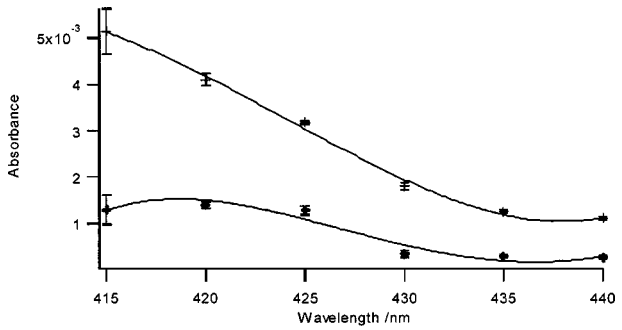

Fig. 2 The absorbance spectrum of Hb bound to the silica surface is displayed for the + bulk concentration 3.88 μM urine/Hb solution and the ● bulk concentration 0.78 μM urine/Hb solution.

3 Results

The UV/vis spectrum for hemoglobin in the control urine sample was measured at a concentration of 3.88 μM. An estimate of the molecular weight of hemoglobin[25] as 64,500 g/mol enables the extinction coefficient ϵ to be determined for each wavelength.

The spectrum of hemoglobin was measured on the surface at two concentrations, (Fig. 2), over the wavelengths 410 to 440 nm. An excitation wavelength of 425 nm was chosen and all further adsorption studies were performed at this fixed wavelength. Lower wavelengths produced a combination of higher error percentages and decreased laser energy output. While the excitation wavelength was not at the center of the absorption peak ($\lambda_{max}=405$ nm), the τ variation ($\sim$1%) and laser power were optimal for the experiment. The extinction coefficient for the absorption wavelength is $\epsilon_{425}=354768\,\mathrm{M}^{-1}\,\mathrm{cm}^{-1}$.

The adsorption isotherm for hemoglobin for known concentrations from 0 to 12 μM is displayed in Fig. 3. Data were collected at varying time intervals and varying concentrations and plotted together. Similar adsorption curves were observed for the varying time intervals (0.5, 2.5, 5, 10, 20, and 30 min). The hemoglobin biofilm formation kinetics evolved over a considerable time period but had reach equilibrium after 30 min. The multilayer hemoglobin biofilm formed from the 30-min time curves are analyzed in this work.

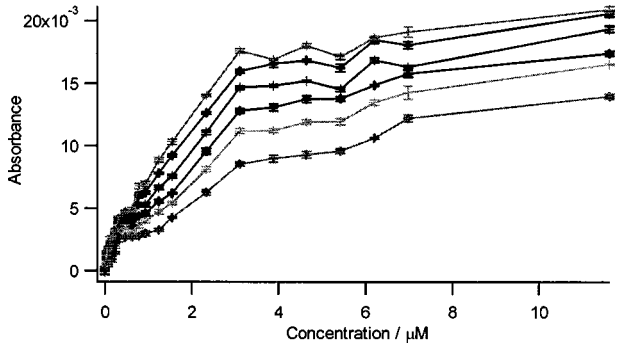

Fig. 3 The residence time study of the Hb solution with the silica surface is shown. The isotherms are plotted in ascending order for 0.5-, 2.5-, 5-, 10-, 20-, and 30-min sampling intervals with the greatest absorbance present at 30 min.

4 Discussion

The formation of a biofilm of the Hb protein on the silica surface is controlled by the packing of the individual protein units in response to the surface charge and the ionic strength of the bulk medium. The silica surface has a surface potential at the pH of the urine sample, pH 7.2, of order -75 mV. The potential arises from the dissociation of the silanol groups on the silica surface with pKa 4.5 and 8.5. Hence, the surface is partially charged.[22,26] The nature of the interface, however, depends on the ionic strength of the bulk solution and shows a variation from a diffuse layer described by the Gouy-Chapman theory to a charged bilayer described by the Stern correction to this theory.[26] The Hb adsorption takes place onto the interface structure, which is competitive with the binding of all positively charged species, such as Na^+ to the surface. The surface potential increases the concentration of ions within the interface due to the Boltzmann factor, and for the silica surface this can enhance the concentration of positive ions (counter ions) by nearly two orders of magnitude and deplete negative (co-ions) by a similar amount.

The biofilm is not restricted to one layer, and subsequent layers may form both on partially filled or complete sublayers. The binding of the protein to the preformed surface thus depends on the sublayer coverage and the binding constant for both Hb to the silica, or the first layer, and to Hb itself in subsequent layers. Further, the binding to each layer may not adopt a close-packed structure characteristic of each cuboid stacking next to one another in the closest configuration. Hence, each layer has a packing stoichometry with a binding model based on a binding constant for the Hb to the silica surface and a second binding constant for subsequent layers. The binding to the first layer is given by:

$$\vartheta_1=\frac{(K_1[\mathrm{Hb}])^{n1}}{1+(K_1[\mathrm{Hb}])^{n1}},$$
$$V_1=\vartheta_1 V_m, \tag{4}$$

where θ_1 is the surface coverage of the silica surface, K_1 is the binding constant for Hb to the silica surface, and n_1 is the binding stoichiometric coefficient for the first layer. The first expression is a binding adsorption isotherm based on the Hill equation,[27,28] which allows for more than one ligand to bind partially to one binding site. For $n_1=1$, this reduces to the competitive binding Langmuir adsorption isotherm. The second expression in Eq. (4) is the concentration Hb in the first layer, with V_m as concentration of molecules at the surface in a complete monolayer. All subsequent layers have binding expressions of the form:

$$\vartheta_i=\frac{(K_i[\mathrm{Hb}])^{n2}}{1+(K_i[\mathrm{Hb}])^{n2}},$$
$$V_i=\vartheta_i V_m, \tag{5}$$

where the binding to subsequent layers has a binding constant different for the binding to silica but similar for all subsequent layers. It is assumed that the transition of Hb protein units between layers is very slow and can be neglected. The Hb protein is cubiod to a first approximation with a base 5×5.5

Table 1 Fitting parameters and constants for the multilayer cooperative binding model.

Fitting parameters	Value ($\mu \pm \sigma$)
Volume of the monolayer/mM	13.30±0.43
Binding constant of Hb to silica	17.32±6.88×10^6 M
Binding constant for Hb to Hb	5.614±0.432×10^5 M
First layer stoichiometry	1.530±0.981
Multilayer stoichiometry	1.792±0.162
Fitting constants	
Refractive index prism 425 nm	1.4677
Excitation wavelength/nm	425
ϵ (420 nm)/M^{-1} cm^{-1}	354, 768
Measured in solution	
Incident angle	72.8 deg
Molecular weight Hb/g mol^{-1}	64, 500
Dimensions[25] of Hb/nm	5×5.5×6.7

nm and a height of 6.7 nm.[25] Each layer within the biofilm is restricted to 6.7 nm, the long dimension of the Hb protein.

The absorbance of the components in the biofilm is calculated using the convolution of the concentration profile with the electric field of the evanescent wave:

$$\text{abs} = \epsilon \int_0^\infty c(z)\exp(-z/d_p)dz, \tag{6}$$

where $c(z)$ is the concentration profile normal to the surface, z is the normal coordinate, d_p is the penetration depth of the evanescent field, and ϵ is the extinction coefficient for Hb at 425 nm. The extinction coefficient is assumed to have the same value as determined for the solution from the UV/vis spectrum. The absorbance is then formally the Laplace transform of the concentration profile.

The parameters in the binding model were fitted to the experimental data for the 30-min exposure using a nonlinear least-squares fitting routine, and the values of the parameters with their one standard-deviation uncertainties are shown in Table 1. The resulting best fit to the experimental data, presented in Fig. 4, is consistent with a multilayer biofilm extending 56 nm into the bulk, as shown in Fig. 5 for the highest Hb concentration, 11.6 μM.

The beam waist of the radiation within the cavity is estimated to be 0.407 mm, which gives a total surface area explored by the evanescent field of 1.3×10^{-3} cm^2 on the surface of the prism. The beam waist is projected as an ellipsoid on the back surface of the prism, but the area of the beam waist is conserved. Assuming the approximate cuboid structure of the Hb protein outlined earlier, and that it binds to the surface with the 5×5.5-nm face on the surface, the total number of Hb proteins within the evanescent field is 4.73×10^9 or

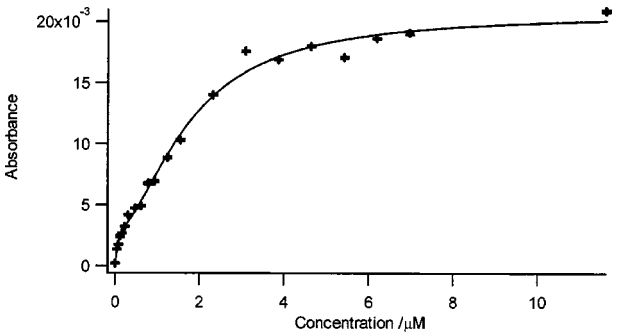

Fig. 4 Adsorption isotherm for Hb onto the silica surface is shown with the best fit line through the data.

7.85 femtomoles within one complete, close-packed monolayer. The depth of a monolayer d_{Hb} is assumed to be 6.7 nm, the vertical height of the protein, giving a maximal concentration on the surface of 9.01 mM. This compares with the value of V_m derived from the fit of 13.30±0.43 mM, suggesting the concentration of molecules at the surface is larger than predicted from the simple calculation, and hence Hb is a smaller cuboid at the surface than the crystal structure measurements. The protein at the surface will be subject to concentrations of NaCl some 100 times greater than the buffer concentrations due to the attraction of Na^+ to the negatively charged surface. The increased electrolyte concentration may have a denaturing effect on the protein. The surface denaturing effect is clearly an important factor in all biofilm formation.

The formation of the Hb biofilm is essentially a "protein tetris" problem, with proteins approaching the surface in random orientations and binding either to the silica side-on or end-on. The chromophore in Hb is, hence, in different orientations at the surface and will have different optical absorbencies. The optical absorbance will also be dependent on the polarization of the radiation leading to a dichroic ratio for *s*- and *p*-polarized light. The random nature of the Hb moieties in the biofilm, however, is unlikely to favor any specific orientation, and the dichroic ratio is likely to be unity. These are measurements for the future.

The Hill equation allows for cooperative binding onto the surface and subsequent layers to allow for proteins to bind differently depending on the orientation of Hb units already present on the surface or higher layers. The binding coefficient for Hb to the first surface layer is $K_1 = 17.32 \pm 6.88$

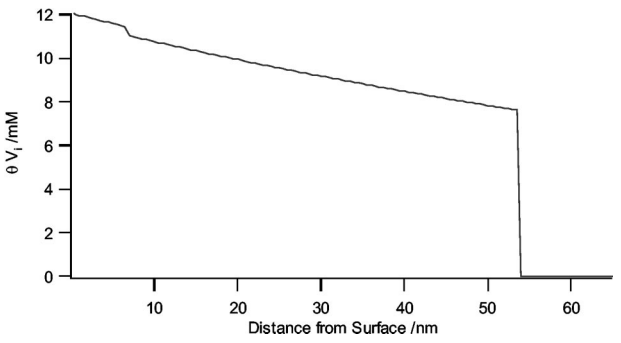

Fig. 5 The concentration profile for 11.6-μM Hb at the silica surface.

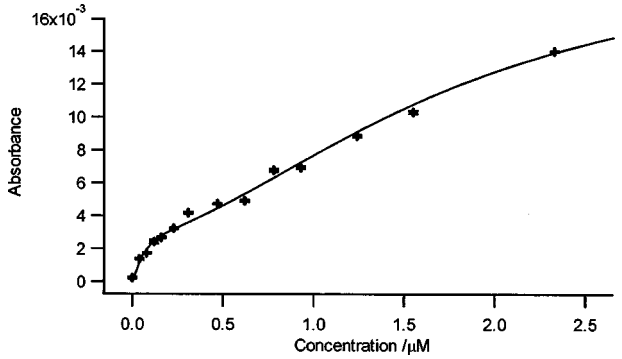

Fig. 6 The low-concentration Hb region of the isotherm is displayed.

$\times 10^6$ M, with a stoichiometry coefficient of $n_1 = 1.530 \pm 0.981$. The errors on these numbers reflect the small contribution of the first layer to the measured isotherm: the lowest concentration observed corresponds to 38% of a completed layer. Subsequent layers are thus better determined with the binding constant $K_2 = 5.614 \pm 0.432 \times 10^5$ M and $n_2 = 1.792 \pm 0.162$.

The concentration profile for 11.6-μM Hb solution concentration is shown in Fig. 5 and extends eight layers into the interface to a total distance of 53.6 nm from the silica surface. The number of layers in the fit was minimized to produce the required absorbance, and the contribution from the bulk concentration beyond eight layers is 3 orders of magnitude smaller than observed. The binding stoichiometry of 1.79 suggests the formation of the bilayer is very dependent on the orientation of the existing Hb units, and displays cooperative binding with nearly two Hb units binding to one unit in a lower layer. The concentration profile shown in Fig. 5 is unlikely to be a unique determination of the biofilm profile, and it is clear from the low-concentration binding characteristics shown in Fig. 6 that the formation of multilayers is immediate and no obvious Langmuir monolayer binding occurs. The exact isotherm and concentration profile will show exposure time dependence, with longer times and higher concentrations forming different layer profiles with different packing characteristics, as shown in Fig. 3. Similar results were observed for the adsorption of lysozyme to the silica surface[29] where at low concentrations the protein aligned along its long axis on the surface, but at higher concentrations a more close packed structure was observed.

5 Conclusions

The adsorption isotherm for Hb is recorded for the silica-water interface when deposited from controlled urine samples. The detection sensitivity for Hb at the surface is of order 2.9 femtomoles, with the minimum detection sensitivity of the instrument allowing concentrations as low as 5.8 nM to be detected. The sensitivity levels observed here are some 2 orders of magnitude better than possible for conventional bench-top optical absorbance assays, and may have important diagnostic consequences for the detection of hemoglobinuria.

A multilayer biofilm is observed and suggested eight layers of packed Hb molecules at larger concentrations. The packed Hb molecules at the surface allow for smaller concentrations to be detected than might be observed for an unpacked solution. The experimental design could be modified into a smaller setup, allowing for portable detection of analytes in biological solutions.

The biofilm concentration profile cannot be unique, but a direct measurement of the biofilm profile may be obtained by a measurement of the absorbance as a function of angle of incidence θ. Hence, from Eq. (6) it would be possible to determine the Laplace transform of the concentration profile as a function of incident angle and recover the profile directly. Similarly, variation of the wavelength will also enable the profile to be deconvolved from the absorbance, although the variation of the extinction coefficient with packing at the surface is assumed to be constant. These measurements must wait for future experiments.

References

1. P. B. Coleman, *Practical Sampling Techniques for Infrared Analysis*, CRC Press, Boca Raton, FL (1993).
2. L. Tolosa, H. Szmacinski, G. Rao, and J. R. Lakowicz, "Lifetime-based sensing of glucose using energy transfer with a long lifetime donor," *Anal. Biochem.* **250**, 102–108 (1997).
3. W. B. Martin, S. Mirov, and R. Venugopalan, "Using two discrete frequencies within the middle infrared to quantitatively determine glucose in serum," *J. Biomed. Opt.* **7**(4), 613–617 (2002).
4. G. Coté, "Noninvasive and minimally invasive optical monitoring technologies," *J. Nutr.* **131**, 1596S–1604S (2001).
5. O. E. Delange, "Losses suffered by coherent light redirected and refocused many times in an enclosed medium," *Bell Syst. Tech. J.* **44**(02), 283–302 (1965).
6. A. O'Keefe and D. A. G. Deacon, "Cavity ring-down optical spectrometer for absorption measurements using pulsed laser sources," *Rev. Sci. Instrum.* **59**, 2544–2554 (1988).
7. G. Berden, R. Peeters, and G. Meijer, "Cavity ring-down spectroscopy: Experimental schemes and applications," *Int. Rev. Phys. Chem.* **19**, 565 (2000).
8. P. Zalicki and R. N. Zare, "Cavity ring-down spectroscopy for quantitative absorption measurements," *J. Chem. Phys.* **102**, 2708 (1995).
9. M. D. Levinson, B. A. Paldus, T. G. Spence, C. C. Harb, J. S. Harris, and R. N. Zare, "Optical heterodyne detection in cavity ring-down spectroscopy," *Chem. Phys. Lett.* **290**, 335 (1998).
10. B. A. Paldus, C. C. Harb, T. G. Spence, B. Wilkie, J. Xie, J. S. Harris, and R. N. Zare, "Cavity-locked ring-down spectroscopy," *J. Appl. Phys.* **83**, 3991 (1998).
11. D. Romanini, A. A. Kachanov, and F. Stoeckel, "Diode laser cavity ring down spectroscopy," *Chem. Phys. Lett.* **270**, 538–545 (1997).
12. J. J. Scherer, J. B. Paul, A. O'Keefe, and R. J. Saykally, "Cavity ring-down laser spectroscopy: History, development, and application to pulsed molecular beams," *Chem. Rev. (Washington, D.C.)* **97**, 25–51 (1997).
13. A. O'Keefe, J. J. Scherer, J. B. Paul, and R. J. Saykally, "Cavity ring-down laser spectroscopy (CRDS): History, development, and applications," *Amer. Chem. Soc. Symp. Ser. 720*, K. W. Busch and M. A. Busch, Eds., ACS, Washington, DC (1999).
14. M. D. Wheeler, S. M. Newman, A. J. Orr-Ewing, and M. N. R. Ashfold, "Cavity ring-down spectroscopy," *J. Chem. Soc., Faraday Trans.* **94**(3), 337–351 (1998).
15. A. C. Pipino, J. W. Hudgens, and R. E. Huie, "Evanescent wave cavity ring-down spectroscopy with a total-internal-reflection mini-cavity," *Rev. Sci. Instrum.* **68**(8), 2978–2989 (1997).
16. A. C. Pipino, J. W. Hudgens, and R. E. Huie, "Evanescent wave cavity ring-down spectroscopy for probing surface processes," *Chem. Phys. Lett.* **280**, 104–112 (1997).
17. A. C. Pipino, "Evanescent wave cavity ring-down spectroscopy for ultra-sensitive chemical detection," *Proc. SPIE* **3535**, 57–67 (1998).
18. A. C. Pipino, "Evanescent wave cavity ring-down spectroscopy: A new platform for thin-film chemical sensors," *Proc. SPIE* **3858**, 74–82 (1999).
19. A. J. Hallock, E. S. F. Berman, and R. N. Zare, "Direct monitoring of absorption in solution by cavity ring-down spectroscopy," *Anal. Chem.* **74**, 1741–1743 (2002).

20. K. L. Synder and R. N. Zare, ''Cavity ring-down spectroscopy as a detector for liquid chromatography,'' *Anal. Chem.* **75**, 3086–3091 (2003).
21. A. M. Shaw, R. N. Zare, C. V. Bennett, and B. H. Kolner, ''Bounce-by-bounce cavity ring-down spectroscopy: Femtosecond temporal imaging,'' *ChemPhysChem* **2**, 118–121 (2001).
22. A. M. Shaw, T. E. Hannon, F. Li, and R. N. Zare, ''Adsorption of crystal violet to the silica-water interface monitored by evanescent wave cavity ring-down spectroscopy,'' *J. Phys. Chem. B* **107**(29), 7070–7075 (2003).
23. L. Hall-Stoodley, J. W. Costerton, and P. Stoodley, ''Bacterial biofilms: From the natural environment to infectious diseases,'' *Nature Rev.* **2**, 95–106 (2004).
24. A. Y. Dergachev and S. B. Mirov, ''Efficient room temperature LiF:F_2^{+**} color center laser tunable in 820 to 1210 nm range,'' *Opt. Commun.* **147**, 107–111 (1998).
25. A. L. Lehninger, D. L. Nelson, and M. M. Cox, *Lehninger Principles of Biochemistry*, 3rd ed., Worth Publishers, New York (2000).
26. A. J. Bard and L. R. Faulkner, *Electrochemical Methods: Fundamentals and Applications*, 2nd ed., Wiley and Sons, New York (2001).
27. K. E. Van Holde, *Physical Biochemistry*, 2nd ed., Prentice Hall, New York (1985).
28. D. G. Kinniburgh, W. H. van Riemsdijk, L. K. Koopal, M. Borkovec, M. F. Benedetti, and M. J. Avena, ''Ion binding to natural organic matter: Competition, heterogeneity, stoichiometry, and thermodynamic consistency,'' *Colloids Surf.* **151**, 147–166 (1991).
29. T. J. Su, J. R. Lu, R. K. Thomas, Z. F. Cui, and J. Penfold, ''The adsorption of lysozyme at the silica-water interface: A neutron reflection study,'' *J. Colloid Interface Sci.* **203**, 419–429 (1998).